the general science journal

Do Periodic Peaks in the Planetary Tidal Forces Acting Upon the Sun Influence the Sunspot Cycle?

Ian R. G. Wilson

Queensland Department of Education, Training and the Arts, Toowoomba, QLD, Australia,
Email: irgeo8@bigpond.com

Abstract

A parameter that is indicative of the peak planetary tidal forces acting upon the Sun i.e. changes in the alignment of Jupiter, at the time of inferior and superior conjunctions of Venus and Earth, naturally exhibits characteristics that either mimic or replicate five of the main properties of the solar cycle. These properties include: the Schwabe cycle; the Hale cycle; the Gnevyshev−Ohl rule; the extended solar cycle; and the sunspot cycle's inherent memory. We believe that this result strongly supports the proposal by Hung (2007) that the solar sunspot cycle is being influenced by variations in the planetary tidal forces acting upon the Sun. This conclusion is supported by the fact that over the last thousand years, every time the peak planetary tidal forces acting upon the Sun are at their weakest there has been a period of low solar activity know as a Grand Solar minimum. The one exception to this rule is a period of weak planetary tidal peaks that roughly coincides with the Medieval Maximum in solar activity. We speculate that this one exception to the rule might have occurred because there was another countervailing factor present during the Medieval Maximum that was working against the planetary tidal effects. We note that the most recent period of weak planetary tidal peaks reached a maximum sometime in the 1990's, without any significant reduction in the level of solar activity. This leads us to conclude that the activity level on the Sun is either in early stages of an Oort−like minimum that will last from 2005−2045, or it is about half way through a period of high solar activity similar to the Medieval Maximum. We believe that evidence pointing towards a significant decrease in the level of sunspot activity in the upcoming solar cycles strongly favors the former conclusion.

1. Introduction

Hung (2007) proposed that the solar sunspot cycle is being influenced by variations in the planetary tidal forces acting upon the Sun. Hung supports his contention by claiming that twenty eight out of the thirty five largest flares on the Sun were observed to start when one or more of the dominant tide-producing planets (Mercury, Venus, Earth and Jupiter) were nearly above ($\leq 10^{O}$) the event positions or at the opposite side of the Sun (180^{O}). He points out that the probability that this could have happened by chance is 0.039 percent.

Hung also notes that the planetary alignment cycles of Venus, Earth and Jupiter exhibits a 11.0 year periodicity that closely matches the timing of the 11 year Schwabe sunspot cycle observed over the last 300 years.

Combining these two pieces of evidence, Hung proposes what is in effect a "mouse−trap" model to explain the variations that are seen in the solar sunspot cycle. In this model, periodic maxima in the relatively insignificant planetary tidal forces affecting the Sun act as the trigger for the release of vast amounts of energy associated with the largest solar flares. The analogy being that the small amount of energy supplied by the paw of a mouse is more than sufficient to release the far greater energy that is stored in the spring of the mouse trap. Hung hypothesizes that the periodic releases of energy during these large flares lead to a resonance interaction between the variations in the peaks in the planetary tidal forces acting on the Sun and the solar cycle. In his "mouse--trap" model, a natural resonance period of 11 years on the Sun (possibly associated with the turn-over time-scale of the meridional flow in the Sun's convective layer) is being driven by a 11 year variation in the strength of the planetary tides.

Hung's "mouse--trap" model would receive added support if it could be shown that variations in the planetary tidal forces acting upon the Sun replicated or mimicked many of the main properties of the sunspot cycle. These properties include: the Schwabe cycle; the Hale cycle; the Gnevyshev−Ohl (G−O) rule; the extended solar cycle; and the sunspot cycle's inherent memory.

In this paper, we will attempt to show that a parameter that is indicative of the planetary tidal forces acting upon the Sun i.e. changes in the alignment of Jupiter, at the time of inferior and superior conjunctions of Venus and Earth, naturally exhibits characteristics that mimic or replicate the five main properties of the solar cycle. In addition, we will propose a simple mechanism that could explain why the planetary alignments of Venus, Earth and Jupiter naturally cause the sunspot cycles to stop or falter, as they do during the Grand Minima.

We begin our arguments with a brief explanation for each of the five main properties of the solar sunspot cycle.

2. The Fundamental Properties of the Sunspot Cycle

A. The Schwabe Cycle

The Schwabe cycle was discovered by Samuel Heinrich Schwabe in 1843, when he noticed that the number of sunspots seen on the Sun's surface increased and then decreased over a period of about 10 years (Schwabe 1843). In reality, the actual cycle length of the Schwabe cycle can vary from about 9 to 14 years (Rogers et al. 2006), although it oscillates about a long-term average value of about 11.1 years (see table 1).

B. The Hale Cycle

George Hale discovered that it takes two Schwabe cycles (or one Hale cycle) for the magnetic polarity of sunspot pairs to reverse and then return to their original state (Hale 1908). This means that fundamental magnetic activity cycle for the Sun is actually 22 years long.

Table 1 shows recent estimates of the mean lengths of the Schwabe and Hale sunspot cycles determined directly from group sunspot numbers (Hoty and Schatten 1998). We can see from the data in table 1 that cycle lengths that are measured from one solar minimum to the next show the least dispersion about a long-term mean. The reason for this, is that it is easier to identify the time of solar minimum more precisely than the time of solar maximum. Indeed, there are some solar maximums that have two distinct peaks (e.g. cycle 23) making it difficult to identify the actual time of maximum solar activity. Hence, the best estimates for the lengths of the Schwabe and Hale cycles from table 1 are 11.1 ± 1.2 years and 22.1 ± 2.0 years, respectively (Rogers et al. 2006, Usoskin and Mursula 2003, Cox 2001).

C. The Gnevyshev−Ohl (G−O) Rule

This rule states that if you sum up the mean annual Wolf sunspot number over an 11 year solar cycle, you find that the sum for a given even numbered sunspot cycle is usually less than that for the following odd numbered sunspot cycle (Gnevyshev and Ohl 1948). The physical significance of the G−O rule is that the fundamental activity cycle of the Sun is the 22 year magnetic Hale cycle, which consists of two 11 year Schwabe cycles, the first of which is an even number cycle (Obridko 1995). While this empirical rule generally holds, there are occasional exceptions such as cycle 23 which was noticeably weaker than cycle 22.

Table 1

Estimates of the Average Length of the Schwabe and Hale Sunspot Cycles.

References	Criteria	Length (yrs)	Cycle	Epoch Covered
Rogers et al. 2006	Min to Min	11.1 ± 1.2	Schwabe	1698.0 to 2008.5
Rogers et al. 2006	Max to Max	10.9 ± 1.9	Schwabe	1705.5 to 2000.3
Usoskin & Mursula 2003	Min to Min	11.0 ± 1.1	Schwabe	1700.0 to 2008.5
Usoskin & Mursula 2003	Max to Max	10.9 ± 2.1	Schwabe	1705.4 to 2000.5
Cox 2001	Min to Min	11.1 ± 1.2	Schwabe	1698.0 to 1986.8
Rogers et al. 2006	Min to Min	22.0 ± 2.0	Hale	1698.0 to 2008.5
Rogers et al. 2006	Max to Max	21.9 ± 2.5	Hale	1705.5 to 1989.6
Usoskin & Mursula 2003	Min to Min	22.1 ± 1.9	Hale	1700.0 to 2008.5
Usoskin & Mursula 2003	Max to Max	21.9 ± 2.5	Hale	1705.4 to 1989.6
Cox 2001	Min to Min	22.2 ± 2.0	Hale	1698.0 to 1986.8

D. The Extended Solar Cycle

Markov and Sivaraman (1989) find that global solar activity for a given sunspot cycle commences at the time of magnetic field reversal, that happens near the sunspot maximum of the previous cycle. They show that the global solar activity includes two main components. The first consists of polar faculae that appear at latitudes of $40 - 70^{O}$ and migrate poleward. The second component consists of the sunspots which show up 5 − 6 years later at latitudes of 40^{O} and then drift equator-ward, giving rise to the butterfly diagram. Markov and Sivaraman (1989) also show that the changes seen in the two components matches the patterns seen in the 5303 Å coronal emission line as well as the excess shear associated with the torsional oscillations.

The concept of an "extended solar cycle" naturally fits into the classic dynamo theory for the sunspot cycle, since the high latitude activity that migrates towards the pole is most likely associated with the poloidal component of the Sun's magnetic field. In the Dynamo theory, the poloidal field that is established just after the polarity reversal at the maximum of the previous solar cycle acts as the seed for the strong toroidal field that is created in the next solar cycle (Sakurai 2000).

The overall picture is one in which the sunspot activity is the main phase of a more extended activity cycle that starts at the solar maximum of the previous cycle and extends for a period lasting roughly 16 to 17 years (Markov and Sivaraman 1989, Wilson et al. 1988, Altrock 1997).

E. The Solar Cycle Memory

There are a number of relationships that involve the use of precursors to predict the peak amplitudes of future sunspot cycles. These include the:

a) **Waldmeier Effect**: This is an observed anti-correlation between the amplitude of a given sunspot cycle and the length of the ascending phase of the cycle i.e. strong cycles reach a maximum in the shortest period of time (Hathaway et al. 2002, Vaquero 2007).

b) **The Amplitude−Period Effect**: This is an anti-correlation between the peak amplitude of a cycle and the length of the preceding cycle, measure from minimum to minimum (Hathaway et al. 2002, Vaquero 2007).

c) **The Amplitude−Minimum Effect**: This is a correlation between the cycle amplitude and the activity level at the previous minimum (Hathaway et al. 2002, Vaquero 2007).

d) **The Drift−Rate Amplitude Correlation**: This is a correlation between the drift velocity for sunspots at the N^{th} cycle maximum and amplitude of the $(N+2)^{th}$ cycle maximum (Hathaway 2006).

Relationships b) and d), in particular, imply that what happens in one solar cycle can affect either the next sunspot cycle or the one after that. This means that any given cycle has a "memory" of what happens in the one or two cycles that immediately proceed it.

Again, the concept of a sunspot cycle memory is a natural outcome of the classic dynamo model that includes the effects of a deep meridional flow in the Sun's convective layer (Dikpati and Charbonneau 1999, Nandy and Choudhouri 2000). In this type of model, the meridional flow during a given sunspot cycle transports residual magnetic flux polar−ward where it acts as the seed for the toroidal field that is created in the next solar cycle (Hathaway 2006).

F. The Grand Minima

C_{14} data from trees and Be_{10} from ice cores (Usoskin et al. 2002, 2003) show that there have been a number of periods in the last 1000 years where the level of solar activity has significantly decreased for periods lasting up to 60−100 years. These Grand minima in solar activity have include the Oort minimum (1010−1050 A.D.), Wolf minimum (1285−1340 A.D.), Sporer minimum (1450−1530 A.D.), Maunder minimum (1645−1715 A.D.) and Dalton minimum (1790−1830 A.D.) (Usoskin et al. 2003).

The two most recent Grand minima are the only ones that have occurred in the era of regular telescopic observations of the Sun. During each of these minima, there has been a dramatic decrease in the number of sunspots seen on the Sun's surface. It is generally assumed that similar decreases in sunspot number took place during the earlier minima.

Despite the near absence of sunspots during the Maunder minimum, a number of researchers (Mursula et al. 2001, Usoskin et al. 2000, 2001, Usoskin and Mursula 2003) have found that the 22 year Hale and 11 year Schwabe activity cycles did not go away during the Maunder minimum, although the effects of the 11 year cycle were substantially reduced. A similar persistence of the 22 year cycle and suppression of the 11 year cycle was found by Miyahara et al. (2005, 2007) for the Sporer minimum.

3. Grand Alignments of Jupiter, Venus and the Earth

One way that we can track the variations in gravitational and tidal forces acting upon the Sun's surface is to note the relative alignment of Jupiter, at the time of inferior and superior conjunctions of Venus and Earth. The quality of Jupiter's alignment with Earth and Venus is simply measured by the position angle of the Sun−Jupiter line with respect to the line joining Venus, Earth and the Sun. If Hung's "mouse−trap" model is correct, then this parameter should exhibit properties that mimic or replicate the main properties of the solar cycle.

The mean sidereal orbital periods of the planets Venus, Earth and Jupiter, measured in days, are (Horizons on-Line Ephemeris System v3.32f May 31 2008):

Venus: T_V = 224.70080 days Earth: T_E = 365.256363 days Jupiter: T_J = 4332.82 days

These sidereal periods produce synodic periods of:

S_{VE} = 583.9214 days = 1.59869 yrs
S_{VJ} = 236.991 days = 0.64885 yrs
S_{EJ} = 398.882 days = 1.09208 yrs

where: S_{VE} = synodic period of Venus−Earth; S_{VJ} = synodic period of Venus−Jupiter; S_{EJ} = synodic period of Earth−Jupiter; and the synodic periods are in Julian years.

This creates a near−resonance condition in the inner solar system such that:

$28 \times S_{VE}$ = 44.7637 years $69 \times S_{VJ}$ = 44.7707 $41 \times S_{EJ}$ = 44.7753 years

The near-resonance conditions mean that if we were to take snap shots of Jupiter's orbital position whenever Venus and Earth aligned with the Sun, we would find that Jupiter comes into a grand alignment with Venus, Earth and the Sun, once every $14 \times S_{VE} = 22.38$ years.

It should be noted, however, that these grand alignments come in two distinct forms. The first is when Jupiter aligns itself with an inferior conjunction of Venus and Earth (i.e. when Venus and Earth are aligned on the same side of the Sun), which we will call inferior alignments. The second is when Jupiter aligns itself with a superior conjunction of Venus and Earth (i.e. when Venus and Earth are aligned on opposite sides of the Sun), which we will call superior alignments.

This means that if we were to start out with an inferior alignment, where Venus, Earth and Jupiter are all aligned on one side of the Sun, 22.38 years later there would be another inferior alignment but this time Jupiter would be on the opposite side of the Sun to Venus and the Earth.

Similarly, if we were to start out with a superior alignment, where Jupiter and Venus are aligned on the same side of the Sun, 22.38 years later there would be another superior alignment but this time Jupiter and Earth would be aligned on the same side of the Sun.

In addition, the superior alignments of Venus, Earth and Jupiter are in anti−phase with the inferior alignments. This means that when we combine the inferior and superior alignments, one form of alignment or another occurs once every 11.19 years.

4. Grand Alignments and the Fundamental Properties of the Solar Cycle

A. The Schwabe and Hale Cycles

Evidence supporting the close synchronization between the grand alignments of Jupiter and the Schwabe and Hale sunspot cycles is provided in figure 1a, 1b, and 1c. These figures show annual sunspot number for the years 1700−1820 (1a); 1800−1920 (1b); and 1900−2004 (1c). Superimposed on each of these plots is a thick curve that indicates the angle between the line joining Jupiter and the Sun and the line formed by the syzygy (alignment) of Venus, the Sun and the Earth at superior conjunction (The Sky Level IV v.5.00). Also superimposed on each of the plots is a dotted curve that indicates the angle between the line joining Jupiter and the Sun and the line formed by the syzygy (alignment) of Venus, Earth and the Sun at inferior conjunction (The Sky Level IV v.5.00). The points on each of these two curves are separated by 1.6 years, corresponding the time between one superior (or inferior) conjunction and the next.

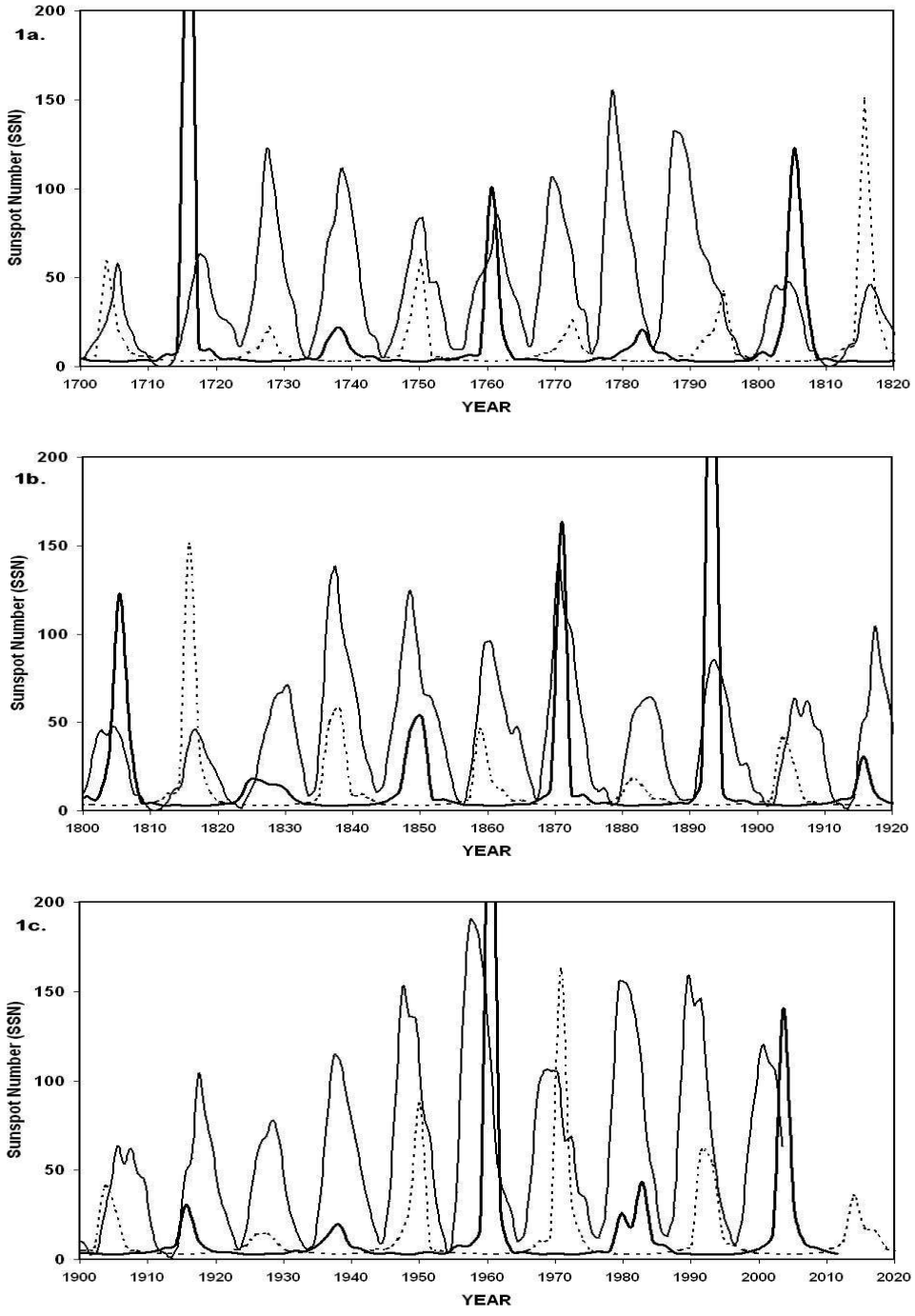

Figures 1a, 1b, and 1c show the annual sunspot numbers for the years 1700−1820, 1800−1920, and 1900−2004, respectively. Superimposed on each of these plots is a thick curve that indicates the angle between the line joining Jupiter and the Sun and the line formed by the syzygy of Venus, the Sun and the Earth at superior conjunction. Also superimposed on each of these plots is a dotted curve that indicates the angle between the line joining Jupiter and the Sun and the line formed by the syzygy of Venus, Earth and the Sun at inferior conjunction. The points on each of these two curves are separated by 1.6 years, corresponding the time between one superior (or inferior) conjunction and the next.

Figures 1a, 1b, and 1c clearly show that the inferior alignments of Jupiter (dotted curve) are separated from the next superior alignment of Jupiter (thick curve) by a time period (11.19 years) that closely matches the long−term mean of the length of the Schwabe cycle (11.1 ± 1.2 years). Note: Jean-Pierre Desmoulins should be acknowledged as the person who originally discovered the close match between the alignment cycles of Venus, Earth and Jupiter and the length of the Schwabe cycle, since he first highlighted this connection in 1989 (Desmoulins 1989).

An indicator of the quality of the synchronization between the average length of the Schwabe cycle and the planetary alignments is provided by the fact that over 300 years (i.e. 1700−2000 A.D.), or 28 Schwabe cycles, the cumulative difference between the times of maximum planetary alignment and maximum sunspot number (SN) only amounts to less than 2−3 years. This means that the difference between the long-term average for the length of the Schwabe cycle and the 11.19 year average time interval between planetary alignments is probably less than or equal to ~ 0.1 years. It is certainly less than ~ 0.2 years since a systematic difference of this size would result in the times of maximum planetary alignment drifting into anti-phase with the Schwabe cycle (~ 5.6 years).

In addition, figures 1a, 1b, and 1c show that each of the superior alignments of Jupiter (peaks on the thick curve) and each of the inferior alignments of Jupiter (peaks on the dotted curve) repeat every 22.38 years. Coupling this with the fact the two types of planetary alignments are in anti−phase with each other, naturally results in planetary alignment cycle that repeats itself on a time scale that matches that of the long−term mean of the Hale cycle (22.1 ± 2.0 years).

B. The Gnevyshev−Ohl (G−O) rule

Figure 2a shows the position angle of Jupiter measured from the alignment axis of the superior conjunction of Venus and Earth plotted against the position angle of Jupiter measured from the alignment axis of the inferior conjunction of Venus and Earth. The inferior and superior conjunctions chosen as the x,y coordinates for each point in this graph are those that are closest to a given solar maximum, for all solar maxima since 1700 A.D. The dates of solar maxima that are used are those published by Usoskin and Mursala (2003).

Figure 2b shows the corresponding plot for position angles of Jupiter at the superior and inferior conjunctions closest to each of the solar minima since 1700 A.D. Again, the dates of solar minima are those published by Usoskin and Mursala (2003). In both figure 2a and figure 2b, symbols have been used to segregate the points into the 14 even and 14 odd numbered solar sunspot cycles.

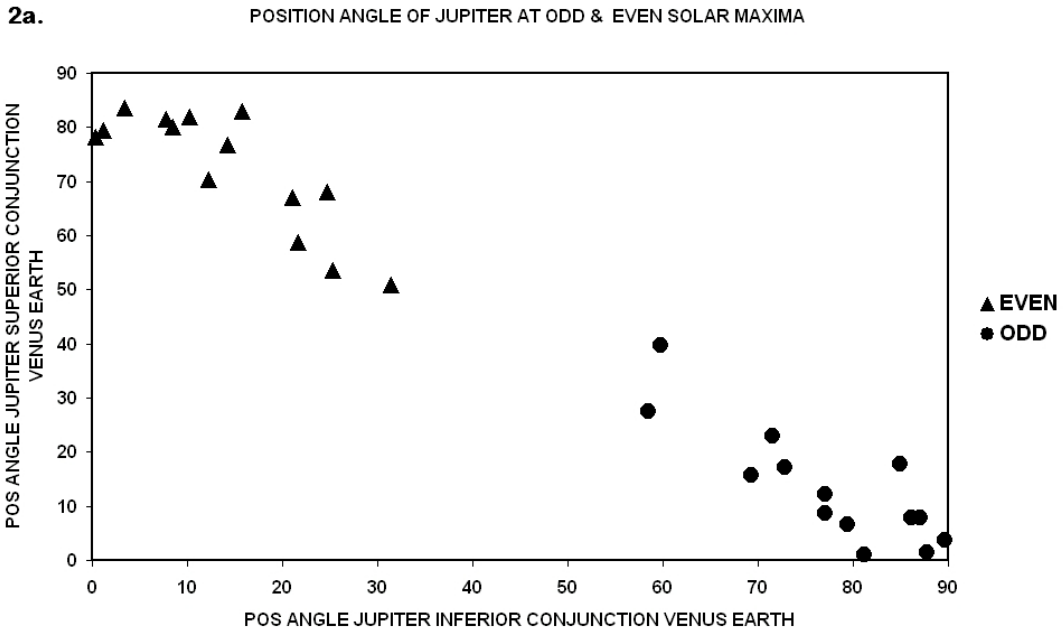

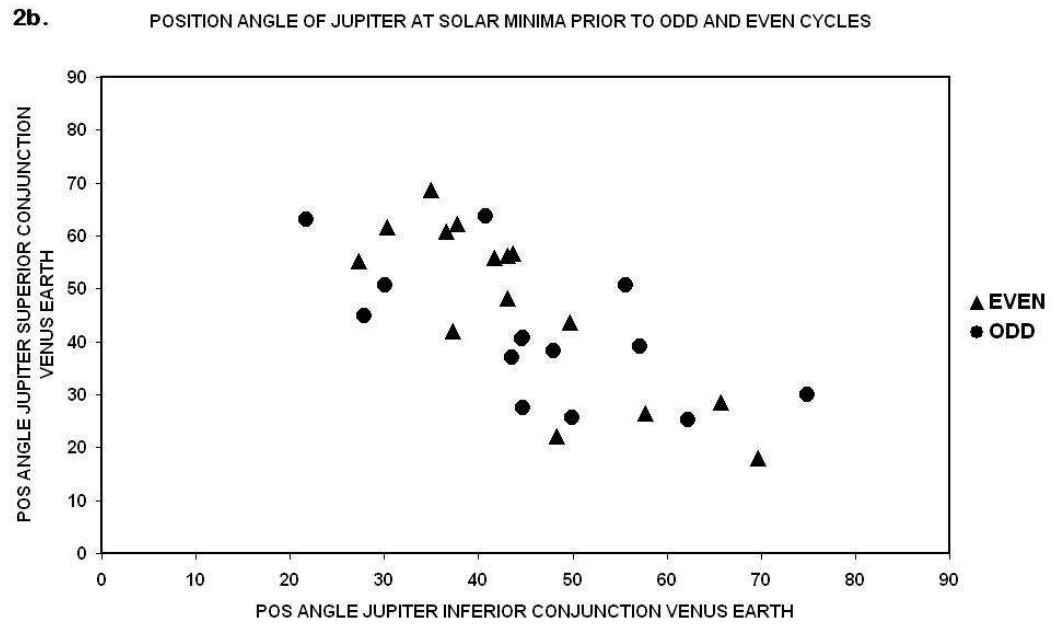

Figure 2a shows the position angle of Jupiter measured from the alignment axis of the superior conjunction of Venus and Earth plotted against the position angle of Jupiter measured from the alignment axis of the inferior conjunction of Venus and Earth. The inferior and superior conjunctions chosen as the x,y coordinates for each point in this graph are those that are closest to a given solar maximum, for all solar maxima since 1700 A.D. Figure 2b shows the corresponding plot for position angles of Jupiter at the superior and inferior conjunctions closest to each of the solar minima since 1700 A.D.

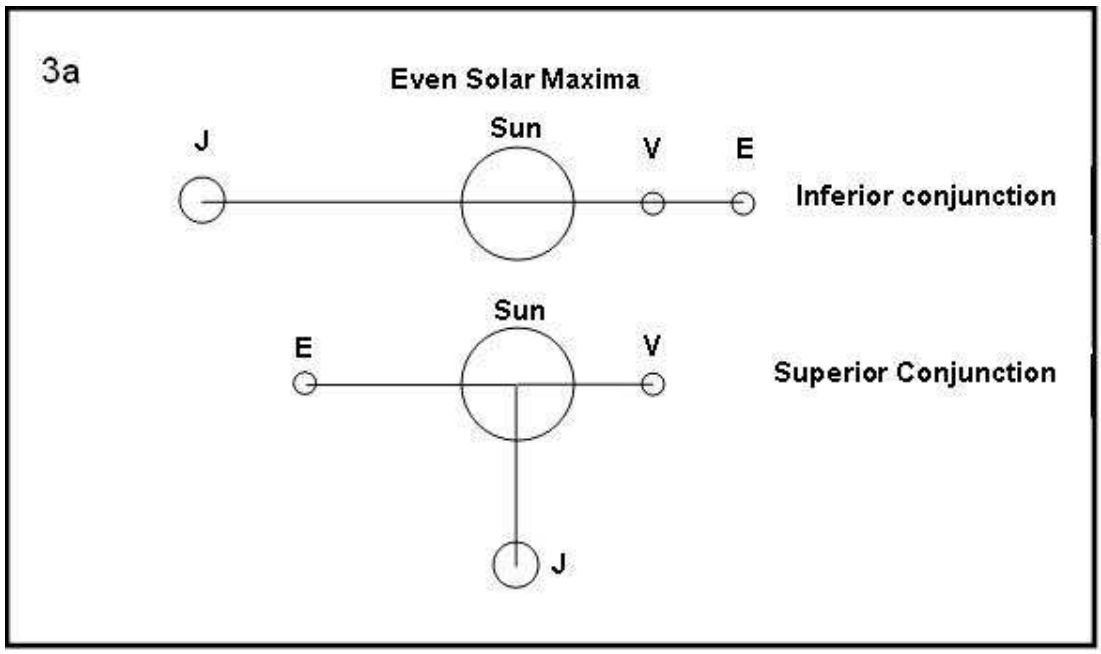

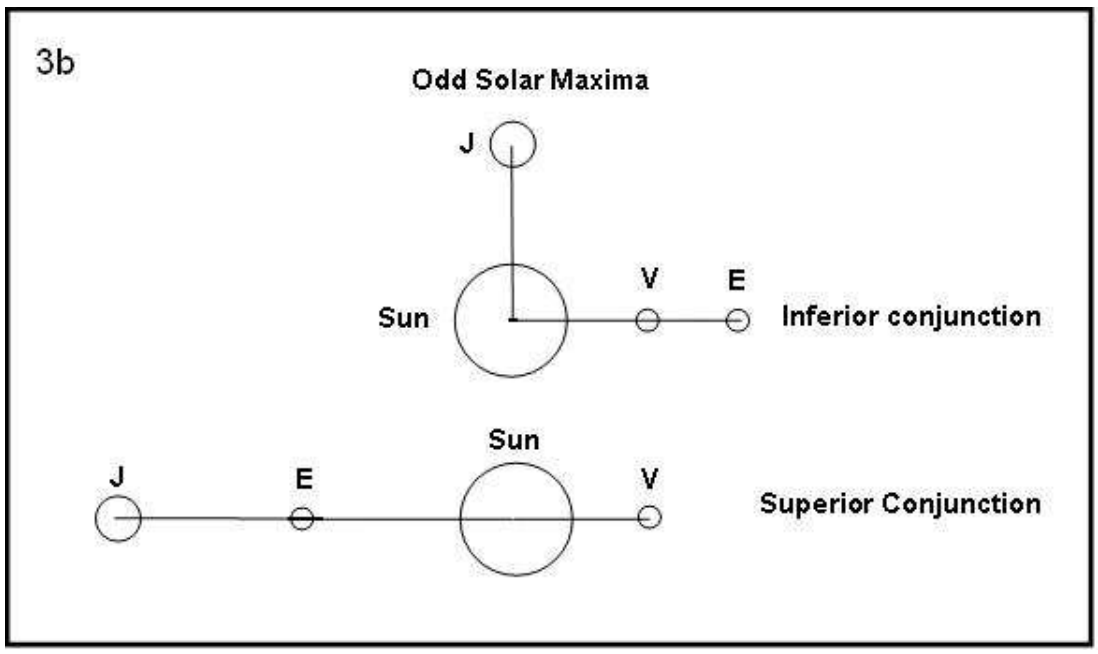

Figure 3a shows Jupiter's position for inferior and superior conjunctions of Venus and the Earth, at times of even numbered solar maxima. Figure 3b shows Jupiter's position at the times of odd numbered solar maxima.

A comparison between figure 2a and 2b shows that there is a marked segregation between the position angles of Jupiter at solar maximum compared to solar minimum. When Venus and the Earth are at inferior conjunction, at a given solar maximum, the position angle of Jupiter either lies between 60^{O} and 90^{O} or 0^{O} and 30^{O}, and when Venus and the Earth are at superior conjunction, for the same solar maximum, the position angle of Jupiter is the complement of that angle. This is in marked contrast with the situation at solar minimum when the position angles of Jupiter lie almost exclusively between 30^{O} and 60^{O} for both inferior and superior conjunctions of Venus and the Earth.

What is even more remarkable, however, is the complete separation between the odd and even cycles at solar maximum that can be seen in figure 2a. This means that Jupiter's position angle, at the time of alignments of Venus, Earth and the Sun, are completely different for even solar maxima than they are for odd solar maxima. Figure 3a shows Jupiter's position for inferior and superior conjunctions of Venus and the Earth, at times of even numbered solar maxima, while figure 3b shows Jupiter's position at the times of odd numbered solar maxima.

The fact that the position angle of Jupiter at the times of even solar maxima is diametrically opposite to those at the time of odd solar maxima raises the possibility that the planetary configuration is related the underlying physical mechanism that is responsible for the G−O rule for solar sunspot maxima. Possible supporting evidence for this conjecture is provided by the instances when the G−O rule has definitely failed.

There have been two pronounced failures of G−O rule. The first, and most dramatic failure, was during sunspot cycles 4 and 5, while the second, less pronounced, failure was during recent sunspot cycles 22 and 23. Each of these sunspot cycles, along with sunspot cycles 3, 14 and 15 have been highlighted in figure 2a. What this data shows, is that G−O rule is more likely to fail at, or soon after, the times when the position angle of Jupiter approaches values that are more typical of solar minimum, rather than solar maximum. Caution needs to be exercised, however, because the position angle of Jupiter during cycles 14 and 15 mimics those of the other cycles that violate the G−O rule, yet these two cycles definitely do not do so.

C. The Extended Solar Cycle

Plotted in figure 4 are the inferior and superior alignment cycles of Jupiter, superimposed on the annual sunspot number for cycles 7, 8, 9 and 10. A detailed look at this plot shows that the actual time between the start of the inferior alignment of Jupiter associated with the even sunspot cycle number 8, and the end of the next superior alignment of Jupiter, associated with the odd sunspot cycle number 9, is 26.4 years. This figure also shows that the 26.4 year period is actually made up of two overlapping cycles, lasting for 16 and 14.4 years, respectively.

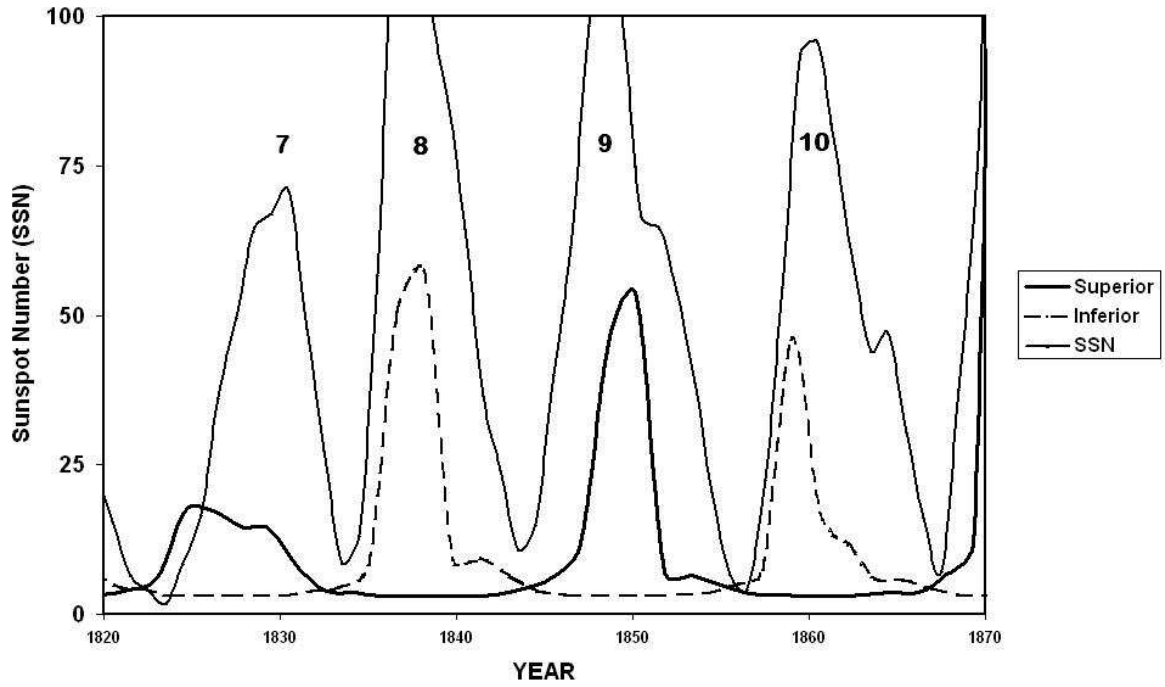

Figure 4 shows the inferior and superior alignment cycles of Jupiter, superimposed on the annual sunspot number for cycles 7, 8, 9 and 10.

Thus, just like the real sunspot cycle, the inferior alignment of Jupiter that is associated with sunspot cycle 8, starts to increase 3.7 years before the minimum at the start of the sunspot cycle 8 in 1833.9. This corresponds to the phase where the polar faculae migrate towards the Sun's pole. This phase is followed by the onset of cycle 8 with sunspots appearing at $\pm 40^{O}$ of latitude and then slowly migrating towards the equator. Finally, the inferior alignment of Jupiter finishes in 1846.2, 16 years after it first started, and 2.7 years after the minimum in sunspot number at the end of cycle 8 in 1843.5.

In like manner, the superior alignment of Jupiter that is associated with sunspot cycle 9, starts to increase 1.3 years before the minimum at the start of the sunspot cycle 9 in 1843.5. This phase is followed by the onset of cycle 9 with the sunspots slowly migrating towards the equator. Finally, the superior alignment of Jupiter finishes in 1856.6, 14.4 years after it first started, and 0.6 years after the minimum in sunspot number at the end of cycle 9 in 1856.0.

Hence, the inferior and superior alignment cycles of Jupiter appear to mimic the behavior of an extended solar sunspot cycle, in that the actual peak planetary alignments can be considered as the main phase of a more extended activity cycle that starts in the previous cycle and extends for a period lasting roughly 16 years.

D. The Solar Cycle Memory

If the solar sunspot cycle is being driven by a mechanism that is associated with the periodic alignments of Venus, Earth and Jupiter, it is very likely that it would take the form of a resonance interaction between the two phenomenon. One indicator of a resonance interaction would be a correlation between the peak strength of the sunspot cycles and the quality of the synchronization of the planetary cycles with the solar activity levels.

Perhaps the best way to measure the synchronization between the solar and planetary cycles is to take the point where one sunspot cycle takes over from its predecessor (i.e. solar minimum) and compare it to the point where the curve for the inferior(/superior) alignment of Jupiter crosses over the curve for the superior(/inferior) alignment of Jupiter. We will call these latter points the planetary alignment cross over points.

Figure 5a shows the peak sunspot number for the $(N+1)^{th}$ cycle plotted against difference between the time of the planetary alignment cross over point and the time of the solar minimum that precedes the N^{th} sunspot cycle. Figure 5b shows the corresponding plot for the peak sunspot number of the N^{th} sunspot cycle, and figure 5c, the corresponding plot for the $(N-1)^{th}$ sunspot cycle.

We can see that in figure 5a there is a weak but definite negative correlation between the peak sunspot number for the $(N+1)^{th}$ cycle and the quality of the synchronization of the planetary and solar cycles at the beginning of the N^{th} cycle. The linear correlation coefficient for the data shown is 0.41, however, the removal of one data point can cause the correlation coefficient to vary between the extremes of 0.30 and 0.52. The linear fit shown in figure 5a is that produced when the point marked by the asterisk is excluded from the fitting process.

Figure 5b shows that there is no correlation between the peak sunspot numbers for the N^{th} cycle and the quality of the synchronization of the planetary and solar cycles at the beginning of the N^{th} cycle (i.e. the linear correlation coefficient = 0.12).

Finally, figure 5c shows that there is a definite positive correlation between the peak sunspot number for the $(N-1)^{th}$ cycle and the quality of the synchronization of the planetary and solar cycles at the beginning of the N^{th} cycle. The linear correlation coefficient for the data shown is 0.58, with the removal of a single data point causing the correlation coefficient to vary between the extremes of 0.55 and 0.61.

5a. (N+1)th Peak SSN vs Synchronization Between the Planetary and Solar Cycles

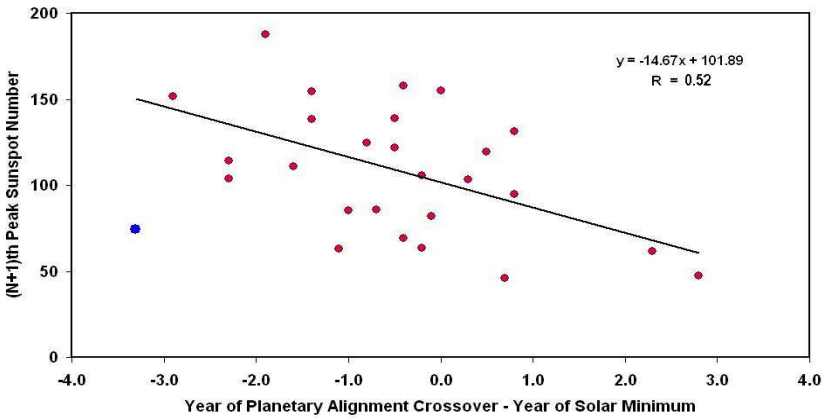

5b. Nth Peak SSN vs Synchronization Between the Planetary and Solar Cycles

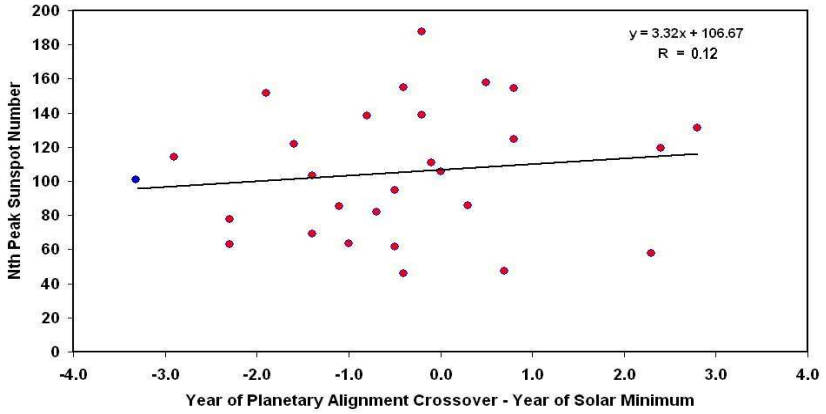

5c. (N-1)th Peak SSN vs Synchronization Between the Planetary and Solar Cycles

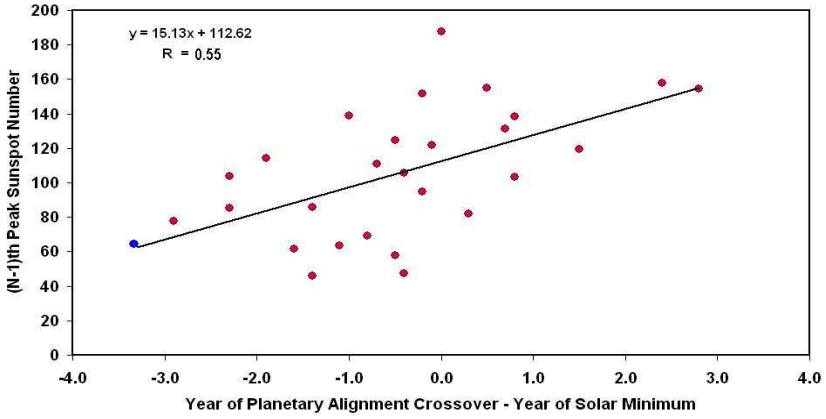

Figure 5a shows the peak sunspot number for the $(N+1)^{th}$ cycle plotted against difference between the time of the planetary alignment cross over point and the time of the solar minimum that proceeds the N^{th} sunspot cycle. Figure 5b shows the corresponding plot for the peak sunspot number of the N^{th} sunspot cycle, and figure 5c, the corresponding plot for the $N-1)^{th}$ sunspot cycle.

Figures 5a, 5b and 5c tell us that there is little or no correlation between the peak sunspot number of the N^{th} sunspot cycle and the quality of the synchronization between the planetary and sunspot cycles. However, there are reasonable correlations between the peak sunspot numbers of the $(N-1)^{th}$ cycle and the $(N+1)^{th}$ cycle and the quality of the synchronization between the planetary and sunspot cycles. This implies that the level of synchronization between the planetary and sunspot cycles at the start of an odd(/even) cycle is correlated with the peak sunspot numbers of the preceding and subsequent even(/odd)sunspot cycles. In essence, this means that any given even(/odd) sunspot cycle has a "memory" of the even(/odd) cycle that proceeded it, much like the drift−rate amplitude correlation rule found by Hathaway (2006) in the actual solar cycle.

Figure 6a further emphasizes the quality of this correlation by showing the difference in peak sunspot numbers of the $(N+1)^{th}$ cycle and the $(N-1)^{th}$ cycle plotted against the level of the synchronization between the planetary and the sunspot cycles. The linear correlation coefficient for the data shown is 0.62, with the removal of a single data point causing the correlation coefficient to vary between the extremes of 0.51 and 0.67.

The high quality of the correlation in figure 6a can be used to make a prediction of the peak annual sunspot number for cycles 24 and 25. If we do this, we obtain 87 ± 11 for the peak annual sunspot number of cycle 24 and 72 ± 8 for cycle 25. The number for cycle 24 uses a planetary alignment cross over point of 1998.8 and a solar minima of 1996.4, while the number for cycle 25 uses a planetary alignment cross over point of 2010.0 and assumes a solar minimum in 2008.5. A peak annual sunspot number of 87 ± 11 for cycle 24 is in good agreement with the predictions of 75 ± 8 made by Svalgaard et al.(2005) based upon the idea that strength of the polar field during the declining phase of one sunspot cycle is a good indicator of the peak sunspot number of the next cycle.

A skeptic might argue that a correlation as good as that seen in figure 6a could also be produced by comparing the timing of sunspot minima with the long−term average length of the Schwabe cycle of 11.1 years. The assumption being that the solar cycle is being driven by an underlying physical mechanism within the Sun that has a fixed period of 11.1 years which just happens to closely match the period of the tidal variations produced by the planets.

Figure 6b shows the difference in peak sunspot numbers of the $(N+1)^{th}$ cycle and the $(N-1)^{th}$ cycle plotted against the difference in years between the date of solar minimum and the nearest multiple of an 11.1 year increment that starts in 1699.0. The starting date of 1699.0 was selected solely because it gives the highest linear correlation coefficient for the chosen data set.

6a.

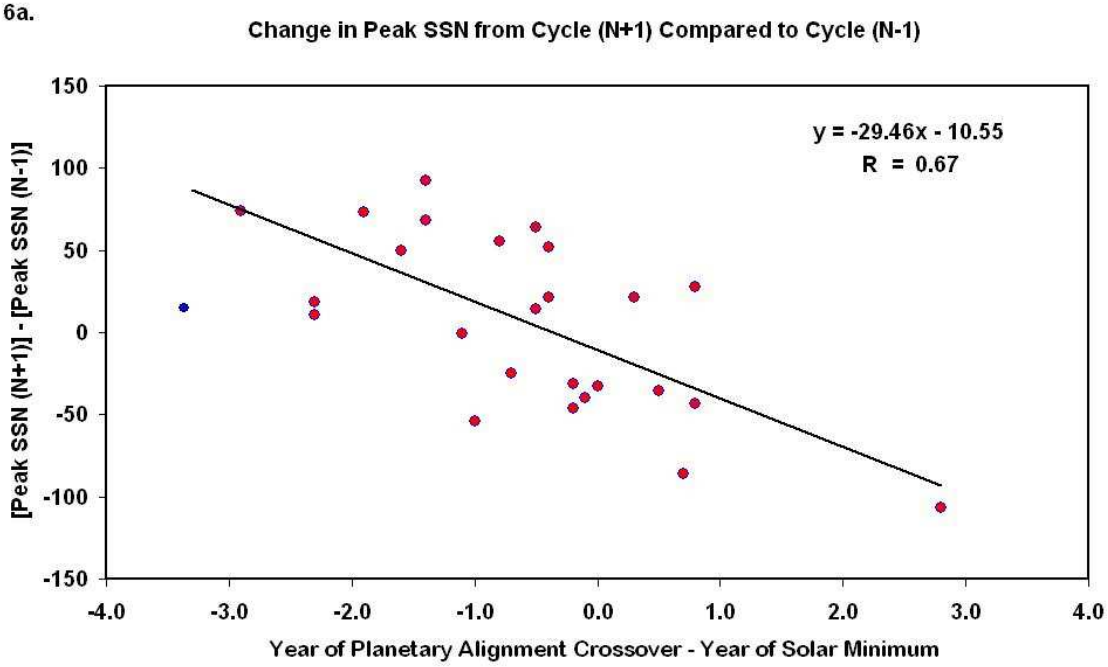

6b.

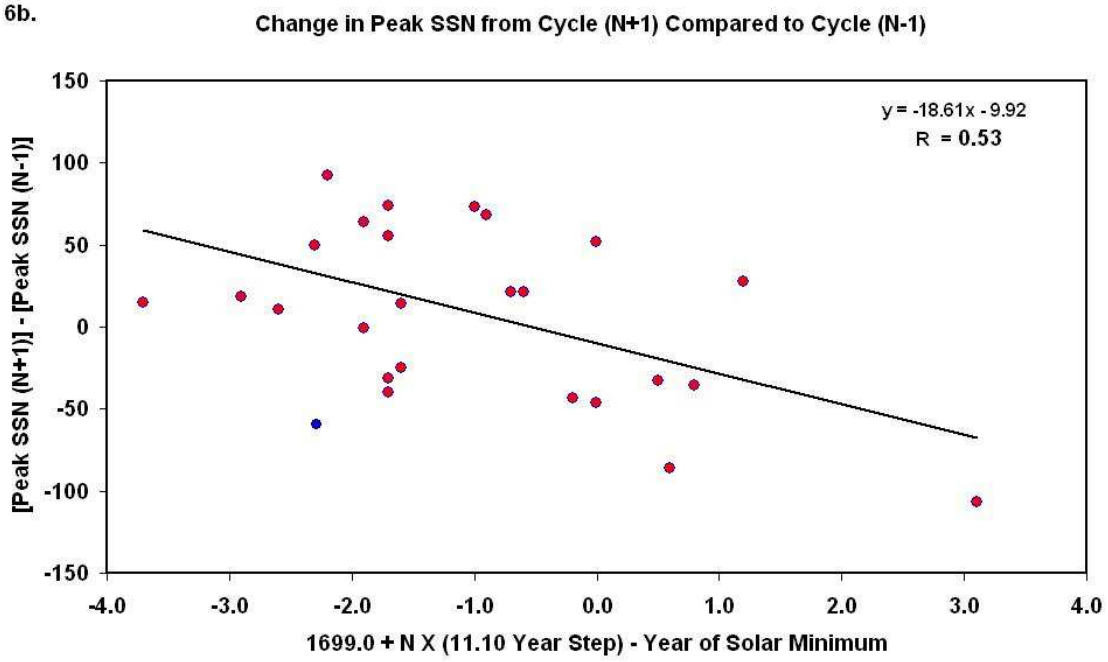

Figure 6a shows the difference in peak sunspot numbers of the $(N+1)^{th}$ cycle and the $(N-1)^{th}$ cycle plotted against the level of the synchronization between the planetary and the sunspot cycles. Figure 6b shows the difference in peak sunspot numbers of the $(N+1)^{th}$ cycle and the $(N-1)^{th}$ cycle plotted against the difference in years between the date of solar minimum and the nearest multiple of an 11.1 year increment that starts in 1699.0.

The linear correlation coefficient for the data shown in figure 6b is 0.47, with the removal of a single data point causing the correlation coefficient to vary between the extremes of 0.30 and 0.53.

The fact is, that we can obtain a much higher correlation coefficient (0.62 vs. 0.47) if we use the difference between the time of solar minimum and the planetary alignment cross over point, than if we use a multiple of a fixed 11.1 year increment. Hence, our result favors the planetary tidal explanation over a mechanism that has a fixed increment of 11.1 years.

5. Are the Grand Minima a Result of Poor Tidal Alignments?

We have shown that the relative alignment of Jupiter, at the time of inferior and superior conjunctions of Venus and Earth, naturally exhibit characteristics that mimic or replicate five of the main properties of the solar cycle. This gives added weight to Hung's contention that the solar sunspot cycle is being influenced by peaks in the planetary tidal forces that are acting upon the Sun (Hung 2007). Hung's planetary tidal model would receive even greater support, however, if it were to explain why there are Grand Minima in the level of solar activity.

Up till now we have used the relative alignment of Jupiter, at the time of inferior and superior conjunctions of Venus and Earth, to provide an approximate representation of the variations in gravitational and tidal force acting on the Sun. However, from this point on we need a more accurate way in which to characterize the quality of the alignments between Venus, the Earth and Jupiter.

In order to improve the accuracy of our knowledge of the quality of the alignments between the planets, we have used the Horizons on-Line Ephemeris System v3.32f kindly provided by the Solar System Dynamics Group at JPL Pasadena California: (URL:http://ssd.jpl.nasa.gov/horizons.cgi; Telnet interface: telnet://horizons.jpl.nasa.gov:6775) to download the heliocentric latitude and longitude of Venus, the Earth and Jupiter at 00:00 UT, for every day between January 1st 1000 A.D. and January 1st 2101 A.D. These latitudes and longitudes were used to determined the subtended angles between each of the planets on any given date.

The point of maximum alignment was determined by finding the minimum of the sum of the subtended angles between Venus and Jupiter, Jupiter and Earth, and Venus and Earth, using the weighting factors 4, 1, and 1, respectively. These weighting factors were chosen to reflect the stronger tidal influences of Venus and Jupiter on the Sun compared to the Earth.

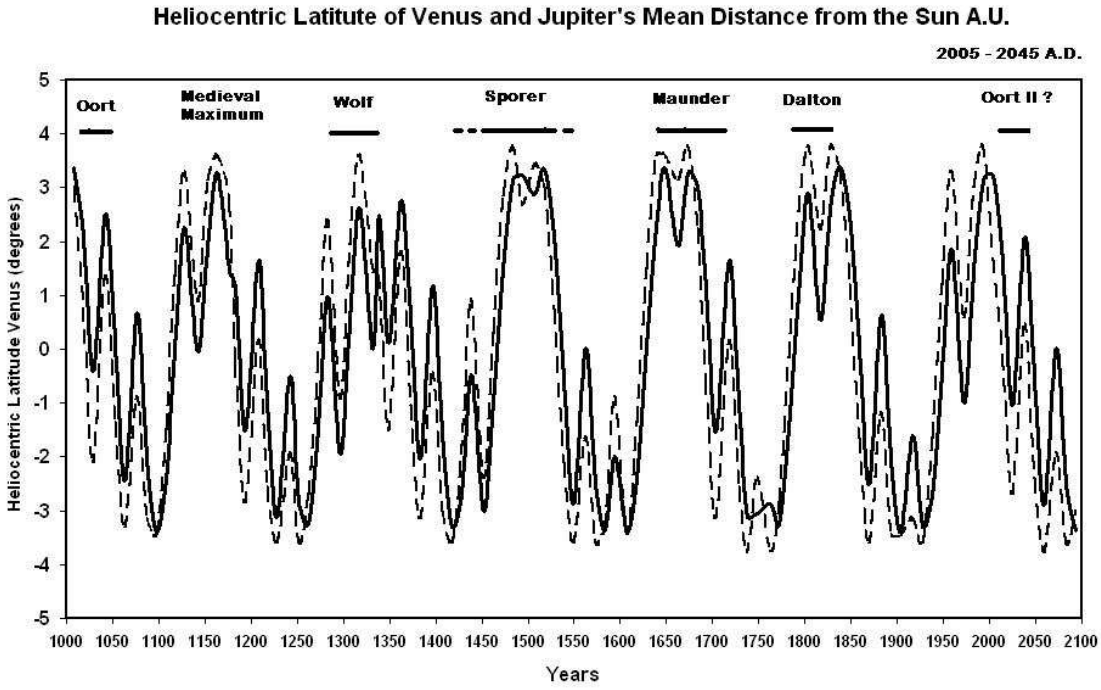

Figure 7 shows the heliocentric latitude of Venus (solid curve) and the mean distance of Jupiter from the Sun in astronomical units (dashed curve), between the years 1000 and 2100 A.D, for each of the points in time where the planetary alignments of Jupiter, Venus and the Earth reach their 11 year maximum. For the purposes of comparison, 5.2 A.U. has been subtracted from the mean distances of Jupiter from the Sun and then the resultant has been scaled to match the amplitude of the variations that are seen in the heliocentric latitude of Venus.

A study of the alignment data reveals that there are two main factors that modulate the strength of the peak planetary tidal forces acting upon the Sun. The first is the 3.3 degree tilt of Venus's orbit with respect to the plane of the ecliptic and the second is the mean distance of Jupiter from the Sun.

Figure 7 shows the heliocentric latitude of Venus (solid curve) and the mean distance of Jupiter from the Sun in astronomical units (dashed curve), between the years 1000 and 2100 A.D, for each of the points in time where the planetary alignments of Jupiter, Venus and the Earth reach their 11 year maximum. For the purposes of comparison, 5.2 A.U. has been subtracted from the mean distances of Jupiter from the Sun and then the resultant has been scaled to match the amplitude of the variations that are seen in the heliocentric latitude of Venus.

We can see from the planetary alignment data in figure 7 that the weakest peak planetary tidal forces occur when Venus is at its greatest positive (most northerly) heliocentric latitude. At these points, Jupiter also happens to be at its greatest distance from the Sun (≈ 5.44 A.U). Similarly,

the strongest peak planetary tidal forces tend to occur when Venus is at a heliocentric latitude of ~ -2.0 degrees. At these points, Jupiter is just over 5.0 A.U. from the Sun.

Marked along the top of figure 7 are the times of the Grand Solar minimum: the Oort minimum (1010−1050 A.D.); the Wolf minimum (1280−1340 A.D.); the Sporer minimum (1450−1530 A.D.); the Maunder minimum (1645−1715 A.D.); and the Dalton minimum (1790−1830 A.D.). Also marked is the Medieval Maximum that extended from roughly 1190 to 1280 A.D. Note: some people argue that the Sporer minimum lasted from 1420 to 1550 A.D. This extension in coverage is represented by dotted lines that bracket the solid line showing the Sporer minimum in figure 7.

Figure 7 shows that every time the peak planetary tidal forces were at their weakest there was a period of low solar activity know as a Grand Solar minimum. The one exception to this rule, was a period of weak planetary tidal peaks centred on 1150 A.D. that spanned the first half of the Medieval Maximum from 1090−1180 A.D. The reason for this discrepancy is unknown, although it could be explained if there was another countervailing factor present during this period that was working against the planetary tidal effects.

Interestingly, figure 7 indicates that the most recent period of weak planetary tidal peaks reached a maximum sometime in the 1990's. Given that we have not yet had a significant reduction in the level of solar activity, we are left with two possible outcomes. It could either mean that we are in for a repeat of an Oort−like minimum that will last from 2005−2045, or it could mean that we about half way through a repeat of period of high solar activity like the Medieval Maximum, that will last from 1920 until about 2100 A.D.

Hence, at this stage, there is some uncertainty as to which of these two outcomes is the most likely. However, there are at least four pieces of evidence that favor another Oort−like minimum.

First, there has been a considerable drop off in the strength of the solar polar magnetic fields, starting at the end of the 1990's (Schatten 2003, Svalgaard et al. 2005). This has been used by Svalgaard et al. (2005) to argue that solar cycle 24 will have a reduced maximum of ~ 75 ± 8.

. Second, there has been a marked reduction in the drift-speed of sunspots during the maximum of cycle 23 (around 2000 A.D.), compared to the maximum of cycle 22 (Hathaway et al. 2006). The reduction in drift rate is believed to be caused by a reduction in the meridional flow rate at the base of the Sun's convective layer. Hathaway et al. 2006 use the Drift Rate−Amplitude correlation to predict a peak sunspot number of ~ 70 for sunspot cycle 25 (peaking in 2023−24).

Third, as of June 2008, it has been more than 12.0 years since the last solar minimum in 1996.4, and there is still no evidence to indicate that we have reached the next minimum. Hence, the peak sunspot number for cycle 24 that is predicted by the Amplitude−Period law (Hathaway 2007) is ~ 81.

Finally, Penn and Livingston (2006) have used high resolution spectral observations of over 900 sunspots from 1998 through 2005 to show that the maximum sunspot magnetic fields have been systematically decreasing at about 52 G yr^{-1}. Using the same data set, they have also shown a concurrent increase in the normalized umbral intensity from 0.60 to 0.75 (corresponding to a black body temperature rise in the sunspots from 5137 to 5719 K). Both of these observations support the contention that, overall, there has been a weakening trend in the level of magnetic activity upon the Sun.

Hence, there are now four pieces of evidence that point towards an upcoming period of reduced solar activity that could start either in cycle 24 or cycle 25. Our result indicates that if this reduction in activity does take place, it will probably herald the start of Oort−like Grand Solar Minimum.

6. Conclusions

We have shown that the relative alignment of Jupiter, at the time of inferior and superior conjunctions of Venus and Earth, naturally exhibits characteristics that mimic or replicate five of the main properties of the solar cycle. These properties include: the Schwabe cycle; the Hale cycle; the Gnevyshev−Ohl (G−O) rule; the extended solar cycle; and the sunspot cycle's inherent memory.

We find that:

A. The inferior alignments of Jupiter are separated from the next superior alignment of Jupiter by a time period (11.19 years) that closely matches the long−term mean of the length of the Schwabe cycle (i.e. 11.1 ± 1.2 years).

B. Each of the superior alignments of Jupiter and each of the inferior alignments of Jupiter repeat themselves once every 22.38 years. Coupling this with the fact the two types of planetary alignments are in anti−phase with each other, naturally results in planetary alignment cycle that repeats itself on a time scale that closely matches the long−term mean of the Hale cycle (i.e. 22.1 ± 2.0 years).

C. The position angles of Jupiter near even solar maxima, with respect to the line joining Venus and the Earth at inferior and superior alignments, are diametrically opposite to the position angles of Jupiter near odd solar maxima. This suggests that the planetary configurations are associated with the underlying physical mechanism that is responsible for the G−O rule for sunspot maxima. Support for this conjecture is provided by the fact that the G−O rule is more likely to fail at, or soon after, the times when the position angle of Jupiter approaches values that are more typical of solar minimum, rather than solar maximum.

D. The inferior and superior alignment cycles of Jupiter appear to mimic the behavior of an extended solar sunspot cycle, in that the actual peak planetary alignments can be considered as the main phase of a more extended activity cycle that starts in the previous cycle and extends for a period lasting roughly 16 years.

E. There is a good correlation ($r = 0.62$) between the difference in the peak sunspot numbers of the $(N+1)^{th}$ and $(N-1)^{th}$ cycles and the difference between the time of the planetary alignment cross over point and the time of the solar minimum that precedes the N^{th} sunspot cycle. This indicates that the level of synchronization between the planetary and sunspot cycles at the start of an odd(/even) cycle is correlated with the peak sunspot numbers of the preceding and subsequent even(/odd) sunspot cycles. In essence, this means that any given even(/odd) sunspot cycle has a "memory" of the even(/odd) cycle that proceeded it, much like the drift−rate amplitude correlation rule found by Hathaway (2006).

These results strongly support Hung's proposal that the solar sunspot cycle is being influenced by variations in the planetary tidal forces acting upon the Sun (Hung 2007).

Hung's tidal force "mouse−trap" model is further supported by the fact that every time the peak planetary tidal forces acting upon the Sun are at their weakest, there is a period of low solar activity know as a Grand Solar minimum. The one exception to this rule, is a period of weak planetary tidal peaks that coincides with the Medieval Maximum. We speculate that this one exception to the rule might have occurred because there were other countervailing factors present during the Medieval Maximum that were working against the planetary tidal effects.

Finally we show that the most recent period of weak planetary tidal peaks reached a maximum sometime in the 1990's. Given that we have not yet had a significant reduction in the level of solar activity, we are forced to conclude that we are either in early stages of an Oort−like minimum in solar activity that will last from 2005−2045, or we about half way through a period of high solar activity similar to the Medieval Maximum, that will last from 1920 until about 2100

A.D. However, we believe that the former conclusion is favored by the increasing amount of evidence that points towards a significant decrease in the level of sunspot activity, starting in cycle 24 or 25.

Acknowledgments

The author would particularly like to thank David Archibald and Bob Foster for their critical feedback and wide ranging comments that have helped hone and distill the quality of the arguments presented in this paper. The author would also like to thank Dr. Brad Carter for his continual encouragement and support for unusual and innovative research at the University of Southern Queensland.

Bibliography

Altrock, R.C., 1997, Solar Phys., 170, 411

Cox, A.N., (ed.) 2001, Allen's Astrophysical Quantities, London, 4th edition, 2nd printing

Desmoulins, J. P., 1989, http://pagesperso-orange.fr/jpdesm/sunspots/sun.html

Dikpati, M. and Charbonneau, P., 1999, Astrophys. J., 518, 508

Gnevyshev, M. N. and Ohl, A. I., 1948, Astron. Zh., 25, 18

Hale, G. E, 1908, Astrophys. J., 28, 315

Hathaway, D. H., 2006, http://solarscience.msfc.nasa.gov/presentations/20060728 NSSTC.ppt

Hathaway, D. H., 2007, http://solarscience.msfc.nasa.gov/presentations/20070216 NSSTC.ppt

Hathaway, D. H., Wilson, R. M., and Reichmann E. J., 2002, Solar Phys., 211, 357

JPL Solar System Dynamics Group (2008) Horizons on-Line Ephemeris System v3.32f 2008, Solar System Dynamics Group, JPL Pasadena California, URL: http://ssd.jpl.nasa.gov/horizons.cgi

Hoyt, D.V. and Schatten, K.H., 1998, Solar Phys., 181, 491

Hung, C−C., 2007, NASA report/TM−2007−214817, available at http://gltrs.grc.nasa.org

Makarov, V.I. and Sivaraman, K.R., 1989, Solar Phys., 123, 367

Miyahara, H., Masuda, K., Menjo, H., Kuwana, K., Muraki, Y., and Nakamura, T., 2005, 29th International Cosmic Ray Conference, Pune, 2, 199

Miyahara, H., Masuda, K., Nagaya, K., Kuwana, K., Muraki, Y., and Nakamura, T. 2007, Advances in Space Research, Vol. 40, Issue 7, 1060

Mursula, K., Usoskin, I.G., and Kovaltsov, G.A., 2001, Solar Phys., 198, 51

Nandy D. and Choudhuri, A.R., 2000, J. Astrophys. Astr., 21, 381

Obridko, V.N., 1995, Solar Phys., 156, 179

Penn, M.J. and Livingston, W., 2006, Astrophys. J. Lett., 649, L45

Rogers, M.L., Richards, M.T., and Richards, D. 2006, preprint, arXiv:astro-ph/0606426

Sakurai, T., 2000, J. Astrophys. Astr., 21, 389

Schatten, K.H., 2003, Advances in Space Research, vol. 32, issue 4, 451

Schwabe, H., 1843, Astronomische Nachrichten, vol. 20., no. 495

Svalgaard, L., Cliver, E.W., and Kamide, Y., 2005, Geophys. Res. Lett., 32, L01104

The Sky Level IV v5.00, Software Bisque Inc.

Usoskin, I.G., Mursula, K., and Kovaltsov, G.A., 2000, Astron. Astrophys., 354, L33

Usoskin, I.G., Mursula, K., and Kovaltsov, G.A., 2001, J. Geophys. Res., 106, 16,039

Usoskin, I.G., Mursula, K., Solanki, S.K., Schüssler, M., and Kovaltsov, G.A., 2002, J. Geophys. Res., 107, 1374

Usoskin, I.G. and Mursula, K., 2003, Solar Phys., 218, 319

Usoskin, I.G., Solanki, S.K., Schüssler, M., Mursula, K., and Alanko, K., 2003, Phys. Rev. Lett., vol. 91, Issue 21, id. 211101

Vaquero, J.M., 2007, Advances in Space Research, vol. 40., issue 7, 929

Wilson, P.R., Altrock, R.C., Harvey, K.L., Martin, S.F., and Snodgrass, H. B., 1988, Nature, 333, 748